Phase-lag distance of OH 83.4-0.9 from eMERLIN and NRT observations

Sandra Etoka[*,1]**, Dieter Engels**[1]**, Eric Gérard**[2]**, Anita Richards**[3]

[1]*Hamburger Sternwarte, DE;* [2] *Observatoire de Paris-Meudon, Fr;* [3] *Jodrell Bank Centre for Astrophysics, UK*
E-mail: sandra.etoka@googlemail.com

OH/IR stars are AGB stars with an optically thick circumstellar envelope of dust and gas commonly exhibiting ground-state OH maser emission at 1612 MHz. With a typical circumstellar-shell extent of 10000 AU (corresponding to 1.25 arcsec at 8 kpc and 0.2 arcsec at 50 kpc) these objects can be used to determine distances throughout the Milky Way and potentially beyond as far as the LMC and SMC via the so-called "phase-lag method". This method combines the linear diameter of the circumstellar shell, obtained from a phase-lag measurement from the variability curves of the maser peaks originating from the back and front sides of the shell, with the shell angular diameter obtained from interferometry. We present here the preliminary results towards the phase-lag distance determination of OH 83.4-0.9 from eMERLIN observations and a NRT (Nancay Radio Telescope) monitoring program. The phase-lag of the red-peak light curve with respect to the blue-peak light curve of this object is 30$\pm$5 days, which equates to a linear diameter of $\sim$5200$\pm$860 AU. The angular diameter of its OH shell is 1.6$\pm$0.2 arcsec, leading to a distance of 3.3$\pm$0.6 kpc.

---

[*]Speaker.

1. Introduction

OH/IR stars are evolved stars on their way to the planetary stage (similarly to the fate of Miras) or the supernova stage depending on their mass. Their mass loss is so copious, reaching for some objects a $\dot{M} = 10^{-4}$ $M_\odot$ yr^{-1} that, contrarily to Miras, their circumstellar envelope (CSE) is optically thick. These objects are mainly detectable through their ground-state OH maser and infrared emission, hence their name. Their OH maser emission is generally strongest in the 1612 MHz line which is characterised by a double-peaked spectrum having a velocity extent of 30 ± 10 km s^{-1}. The vast majority are periodic objects, with periods ranging typically between 1 to 6 years. The typical diameter of their OH CSEs is 2000 to 10000 AU, meaning that there are sizeable objects even at the Galactic-Center and Large-Magellanic-Cloud distances (LMC), with up to angular diameters of 1.25 arcsec and 0.2 arcsec, respectively. Since they can be found throughout the entire Galaxy and have been detected in the LMC (Marshall et al. 2004), this makes them potentially valuable objects for distance determination in the Galaxy itself and beyond, towards the Local Group of galaxies (Etoka et al. 2015). Nonetheless, since these objects are optically thick, determination of their distances via optical parallax measurements is not possible. As stars do not strictly follow the Galactic rotation, kinematic distances can be imprecise by up to a factor of 2 (Reid et al. 2009). The period-luminosity relation found towards Miras (Whitelock et al. 1991) breaks down for P> 450 days. VLBI astrometry has been successfully used to measure parallaxes towards Miras (with OH masers: e.g., Vlemmings & van Langevelde 2007) in the solar vicinity (i.e., D< 2kpc) and towards more distant so-called "Water Fountain" sources (with H$_2$O masers: e.g., Imai, Sahai & Morris 2007) but this technique has not been tried yet on OH/IR stars. Another promising technique to infer reliable distances from OH/IR is the "phase-lag method".

2. Phase-lag distance method

Determining distances via the phase-lag method relies on the combination of the linear and angular diameter measurements of the CSE of a given OH/IR star, which can be independently retrieved. OH/IR stars typically exhibit a double-peaked spectral profile where the blueshifted peak ("blue" peak here after) emanates from the front cap of the CSE, the redshifted peak ("red" peak here after) emanates from the back cap of the CSE, and the faint interpeak emission emanates from the outer part of the CSE. To recover the linear diameter of the shell, this requires the objects to have a periodically variable OH emission. It relies on the travel-time difference between the front and back cap of the shell, which is directly measured by the "phase-lag" of the red-peak light curve with respect to the blue-peak light curve. Since OH/IR stars are long-period objects, retrieving such information requires a long-term, well-sampled monitoring of their OH maser emission. The angular diameter is retrieved from interferometric mapping. Since the outer part of the CSE is sampled by the faint inner portion of the spectrum, to obtain the most faithful extent of the shell requires good sensitivity so as to retrieve as much signal as possible close to the stellar radial velocity, corresponding to the central velocity of the spectral profile. The proof of concept of phase-lag measurements was performed in the 1970's (Schultz, Sherwood & Winnberg 1978). A systematic exploration of the phase-lag method to retrieve distances from OH/IR stars was performed as early as the 1980's (Herman & Habing 1985; van Langevelde et al. 1990) This method relies heavily

on the assumption that the CSE is a spherically thin shell in uniform radial expansion. Deviation from this assumption, unless corrected by a proper geometrical modelling of the shell, can lead to distance uncertainty $> 20\%$ (Etoka & Diamond, 2010).

3. Modus operandi

We have been monitoring the maser emission of 20 OH/IR stars on a monthly basis for 7 years now at the Nançay Radio Telescope (NRT) with a sensitivity of 100 mJy and a velocity resolution of 0.035 km/s. Half of the sample is composed of sources for which phase-lags have already been determined by Herman & Habing (1985) and van Langevelde et al. (1990), while the second half of the sample is composed of new sources for which the phase-lags are measured for the first time. Amongst the sources of the first half, some sources are comparison stars used to verify the phase-lags reported, while for the rest of the sources (common between the two 1980's afore-mentioned works), the aim is to redetermine the phase lags, as the reported phase lags were inconsistent with each other.

To find out the phase lag (τ_0) of a source, we construct its 1612 MHz blue-peak and red-peak light curves F_b, F_r respectively, by integrating the maser emission on the entire blueshifted and redshifted parts of its velocity profile. Assuming that both maser lightcurves are similar, that is, the only difference between the two is their mean flux and the amplitude of their variation, we can determine τ_0 of the red-peak light curve with respect to the blue-peak light curve by minimising the function $\Delta F = F_r(t) - a \cdot F_b(t - \tau_0) + c$ (where a and c are constants) so as to match the difference in amplitude and mean flux of the two maser light curves.

For the sources for which interferometric mappings exist in the literature, we used these to infer their angular diameter and hence make a first estimate of their distance, knowing that these will need refinement via future more sensitive mapping to retrieve more faithful angular diameters. We have started an imaging campaign of the sources of our sample with the Jansky VLA and eMER-LIN, during the maximum of their light curve. Engels et al. (2014) present the preliminary results of the first measurement of the distance of OH $16.1 - 0.3$, another source for which no angular diameter existed, via the phase-lag method (and based on VLA mapping), along with the status of the overall project so far.

4. Results

Here we present the preliminary results of the linear and angular diameter determinations of the CSE of OH 83.4-0.9, leading to the first measurement of its distance via the phase lag method. It is based on our NRT monitoring (cf. section 3) and eMERLIN observations performed in February 2014. The eMERLIN observations have a spectral resolution of 0.17 km s^{-1}, and a sensitivity of 14 mJy beam^{-1} per channel.

4.1 Linear diameter determination

The left side of Figure 1 presents the blue- and red-peak light curves obtained from the NRT monitoring towards OH 83.4-0.9 for the 7-year period 2008-2014. The velocity ranges used to construct these 2 light curves are $[-59.0; -38.5]$ km s^{-1} for the blue-peak light curve and $[-38.5; -18.0]$ km s^{-1} for the red-peak light curve. The right-hand side of Figure 1 presents the best fit, performed following the method explained in Section 3. This leads to a phase-lag of the red-peak light curve with respect to the blue-peak one of 30$\pm$5 days, which equates to a linear diameter of $\sim$5200$\pm$860 AU.
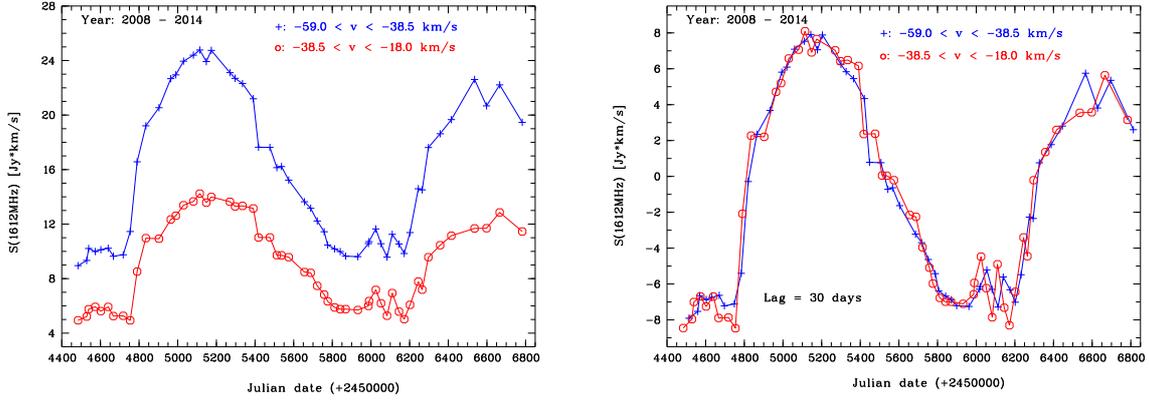
Figure 1: Left: blue-peak and red-peak light curves of OH 83.4-0.9 obtained from the NRT monitoring for the 7-year period 2008-2014. The velocity ranges used to construct these 2 light curves are given in the upper-right side of the figure. **Right:** Best estimation of the phase lag obtained following the method presented in section 3.

4.2 Angular diameter determination

The assessment whether the simple assumption of a spherically-thin shell in uniform radial expansion is valid for this source was made thanks to the channel maps obtained from the final eMERLIN dataset. These are indeed consistent with such assumption. Moreover, the comparison of the eMERLIN final dataset spectrum with the single-dish spectrum obtained with the NRT $\sim$3 weeks after the eMERLIN observations comfirms that we recovered all the signal, especially the faint inter-peak signal corresponding to the outer part of the shell (cf. Fig 2).

In Figure 3 we present the map obtained from the integration of the channels sampling the inner part of the spectrum covering the velocity range $\sim[-55; -23]$ km s^{-1} which gives the best render of the extent of the shell. The magenta full and dotted circles delineate the outer part of the shell. From this, we inferred an angular diameter of 1.6$\pm$0.2 arcsec. Combining this with our linear diameter determination of the source via phase-lag measurements (cf. Section 4.1) leads to a distance determination of 3.3$\pm$0.6 kpc for OH 83.4-0.9.
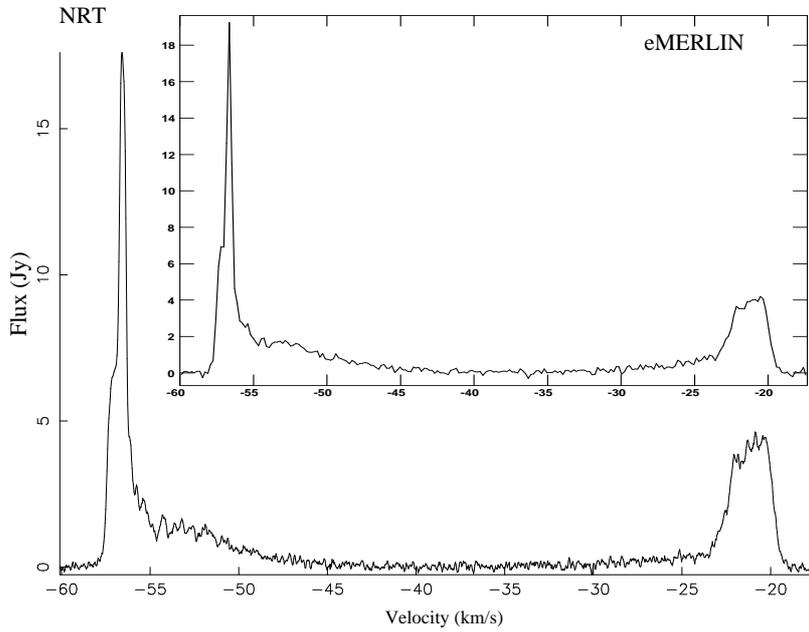
Figure 2: **Main panel:** NRT spectrum taken ~3 weeks after the eMERLIN observations. **Insert panel:** eMERLIN final dataset spectra. Note the difference of spectral resolution between the 2 spectra (0.035 $\mathrm{km\,s^{-1}}$ for the NRT spectrum against 0.17 $\mathrm{km\,s^{-1}}$ for the eMERLIN one.
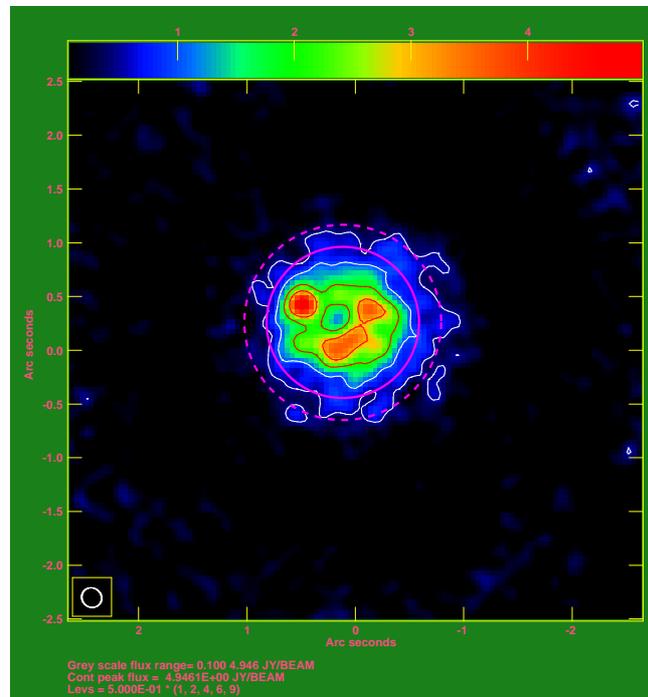
Figure 3: eMERLIN map obtained from the integration of all the channels of the inner part of the spectrum covering the velocity range ~$[-55; -23]$ $\mathrm{km\,s^{-1}}$. The magenta full and dotted circles delineate the outer part of the shell.

5. Summary

We have presented here the preliminary results of the determination of linear and angular diameter of OH 83.4-0.9 based on our NRT monitoring program and eMERLIN observations, respectively. Using the phase-lag method, we determine a distance of 3.3±0.6 kpc for this object. Our projects comprise 20 objects in total for which phase lag distances will be measured. The aim of the project is to improve the angular diameter determination of the objects for which imaging has already been done in the past but with a lower sensitivity that is currently achievable with the VLA and eMERLIN, the 2 interferometers the most suited in terms of sensitivity and resolution for the objects of our sample. In particular, the sensitivity achieved by these instruments render the detection of the faint inter-peak signal possible, which will allow us not only to retrieve more reliable angular diameter measurements but also, to better constrain the shell (a)symmetry, both parameters being crucial for reliable phase-lag distance determinations. Ultimately, we are aiming at constraining the distance uncertainties of the phase-lag distance method itself.

Acknowledgments

References

[1] Engels D., Etoka S., Gérard E., Richards A.M.S., 2014, Proc. of "Why galaxies care about AGB stars III", Eds. F.Kerschbaum, J. Hron & B. Wing *(in press)*

[2] Etoka S., Engels D., Imai I. et al., 2015, Proc. of "Advancing Astrophysics with the Square Kilometre Array", PoS(AASKA14)125, *in press*

[3] Etoka S. & Diamond P.J., 2010, MNRAS 406, 2218

[4] Imai H., Sahai R. & Morris M., 2007, ApJ 669, 424

[5] Herman J., Habing H.J., 1985, A&AS 59, 523

[6] Marshall J.R., van Loon J.T., Matsuura M. et al., 2004, MNRAS 355, 1348

[7] Reid M.J., Menten K.M., Zheng X.W. et al., 2009, ApJ 700, 137

[8] Schultz G.V., Sherwood W.A., Winnberg A., 1978, A&A 63L, 5

[9] van Langevelde H.J., van der Heiden R., van Schooneveld C., 1990, A&A 239, 193

[10] Vlemmings W.H.T. & van Langevelde H.J., 2007, A&A 472, 547

[11] Whitelock P., Feast, M., Catchpole R., 1991, MNRAS 248, 276